Supplementary Information

Table S1: Rearrangements by chromosome

Neanderthal	1	122
	2	172
	3	61
	4	111
	5	31
	6	19
	7	202
	8	27
	9	122
	10	132
	11	66
	12	22
	13	48
	14	31
	15	69
	16	145
	17	133
	18	44
	19	36
	20	110
	21	107
	22	27
	X	35
	Y	98
Denisovan	1	128
	2	252
	3	99
	4	180
	5	36
	6	43
	7	283
	8	39
	9	119
	10	233
	11	82
	12	58
	13	28
	14	37
	15	67
	16	215
	17	124
	18	73
	19	66
	20	132
	21	136
	22	39
	X	79
	Y	112

Table S2: Overrepresented Gene Ontology Categories

Genome	function	EASE
Altai Neanderthal	flotillin	1.27
Denisovan	keratin	1.28
	microtubule	1.17
	flotillin	1.14
	fibronectin	1.13

Table S3: Genes with $d_N/d_S > 1.0$

Genome	Gene	d_N	d_S	d_N/d_S
Altai Neanderthal	ENSG00000214681	0.003584	0.000004	999.0[1]
	ENSG00000184276	0.006455	0.000006	999.0[1]
	ENSG00000186146	0.000002	0.000000	134.7
	ENSG00000062096	0.004416	0.000004	999.0[1]
	ENSG00000203780	0.000001	0.000001	1.2
	ENSG00000132196	0.001461	0.000007	221.1
	ENSG00000142794	0.005703	0.004413	1.3
Denisovan	ENSG00000184276	0.006455	0.000006	999.0[1]
	ENSG00000203780	0.000001	0.000001	1.2
	ENSG00000178852	0.004800	0.000044	109.7
	ENSG00000196757	0.001320	0.000018	73.6

[1] 999.0 is the highest ratio of d_N/d_S that PAML reports. These results may be driven by the low estimates of d_S. There is no clear signature of misalignment in the data.

Table S4: Mean coverage in properly paired reads by chromosome

Neanderthal	1	3.03442
	2	3.11308
	3	3.072
	4	3.21629
	5	3.11201
	6	3.17608
	7	3.09368
	8	3.17866
	9	3.00747
	10	3.17219
	11	2.96935
	12	2.99443
	13	3.16641
	14	3.02113
	15	2.93645
	16	2.99368
	17	2.77537
	18	3.08382
	19	2.58384
	20	2.78167
	21	3.23365
	22	2.56239
	X	3.16043
Denisovan	1	3.03442
	2	3.11308
	3	3.072
	4	3.21629
	5	3.11201
	6	3.17608
	7	3.09368
	8	3.17866
	9	3.00747
	10	3.17219
	11	2.96935
	12	2.99443
	13	3.16641
	14	3.02113
	15	2.93645
	16	2.99368
	17	2.77537
	18	3.08382
	19	2.58384
	20	2.78167
	21	3.23365
	22	2.56239
	X	3.16043

Table S5: Y Coverage

Genome	Locus	Mean Coverage	Median Coverage	Standard Deviation
Neanderthal	whole Y	0.91	0	18.5
	within 1kb of Y-translocations	74	14	220
Denisovan	whole Y	0.56	0	12.5
	within 1kb of Y-translocation	52	7	160

Table S6: Human immortalized cell lines used to confirm rearrangements

Cell line
HGDP00521
HGDP00542
HGDP00665
HGDP00778
HGDP00927
HGDP00998
HGDP01029
HGDP01284
HGDP01307
HGDP0456

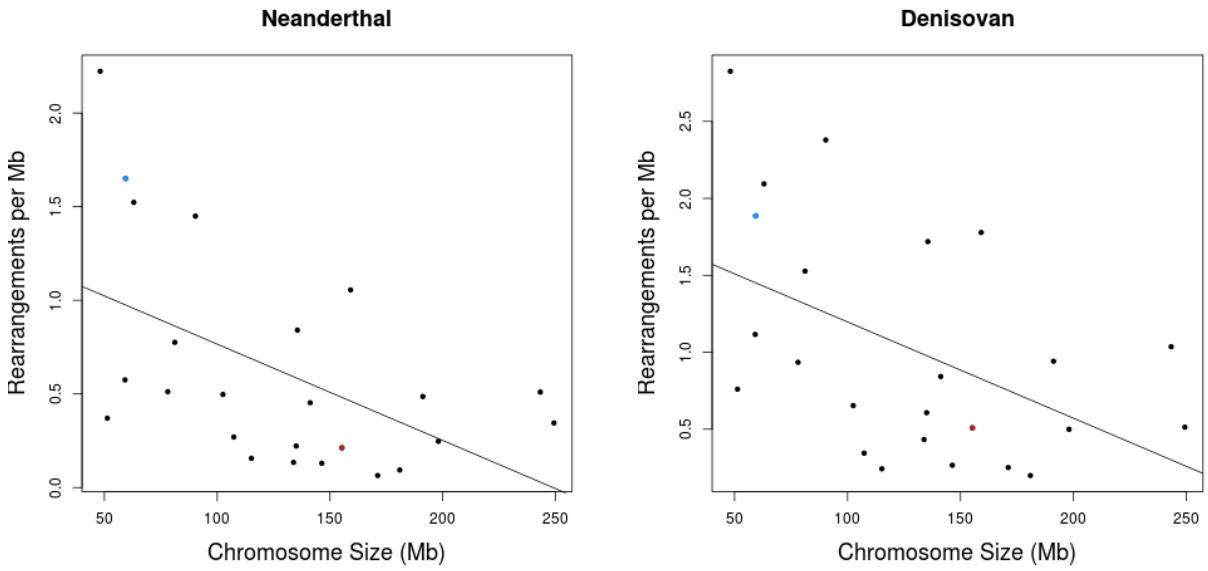

(A) (B)

Figure S1: Incidence of rearrangements vs chromosome size for (A) Neanderthal and (B) Denisova. Both samples show a significant negative correlation between the rate of rearrangement and chromosome size (Neanderthal $R^2 = 0.24$, $P = 0.0088$; Denisovan $R^2 = 0.20$, $P = 0.016$). These results may suggest that ectopic recombination is more common for small chromosomes or that small chromosomes are degenerating. Rates of rearrangements are higher in Denisovan than Neanderthal, but chromosomes show consistent patterns across the two species. The X chromosome (red) does not appear to have an excess of rearrangements given its size, but the Y chromosome (blue) carries a large number of rearrangements per basepair, especially considering that there is no Y chromosome sequence present in these female individuals.

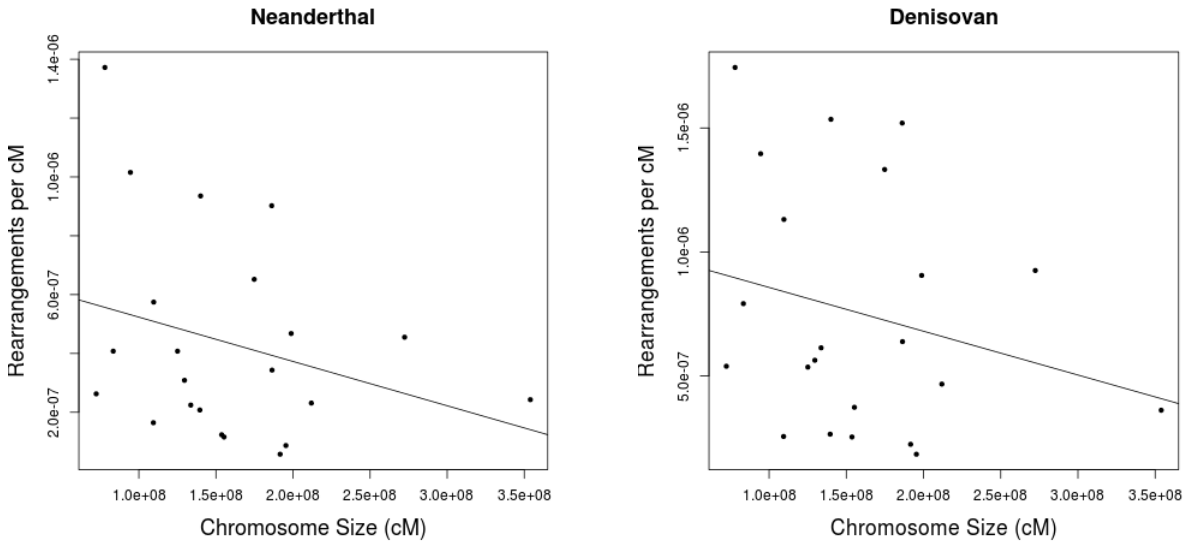

(A) (B)

Figure S2: Rate of rearrangements vs chromosome size in centimorgans for (A) Neanderthal and (B) Denisova. There is no significant correlation between the rate of rearrangement and chromosome size (Neanderthal $R^2 = 0.036$, $P = 0.195$; Denisovan $R^2 = 0.01$, $P = 0.28$).

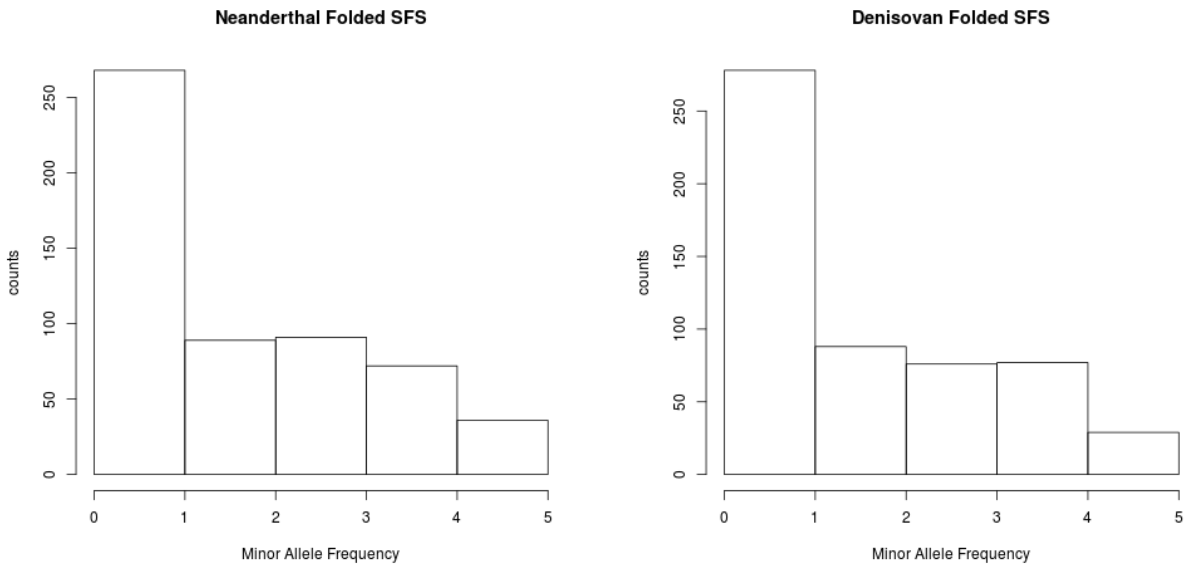

(A) (B)

Figure S3: Folded presence-absence spectrum for genome structure changes identified in (A) Neanderthal and (B) Denisovan genomes assayed in a population of 10 individual modern humans. The presence-absence spectrum indicates a skew toward high and low frequency variants with fewer moderate frequency variants. There is no significant difference between the folded mutation spectrum for rearrangements identified in Neanderthals vs. Denisovan.

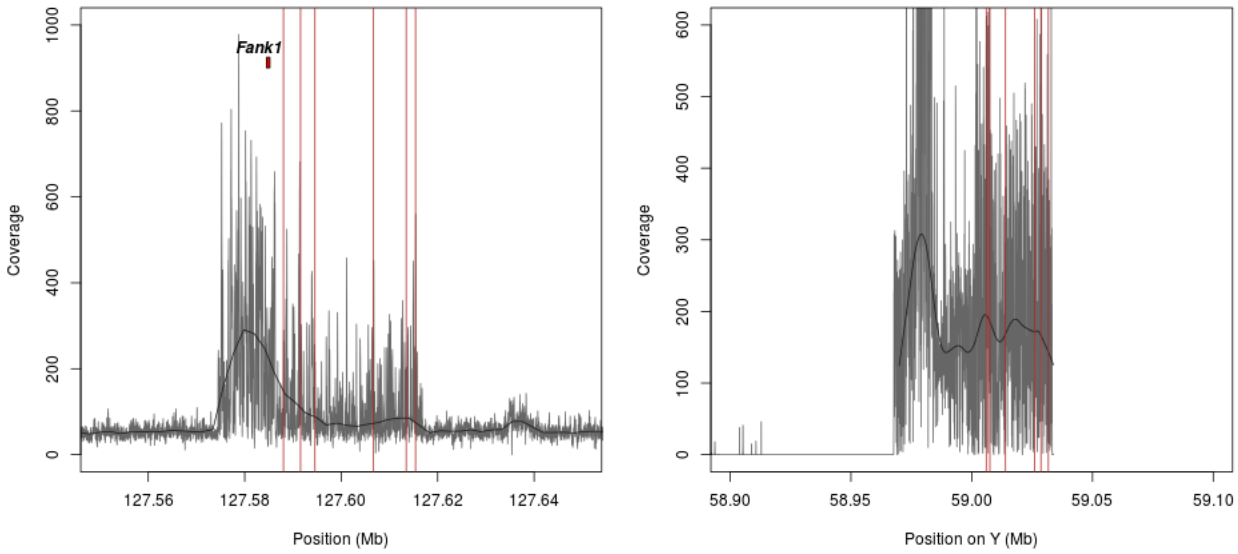

(A) (B)

Figure S4: Genomic coverage with lowess smoothed regression line at the site of a rearrangement (A) at the *Fank1* locus and (B) on the translocated segment of the Y in the Altai Neanderthal. Locations of abnormally mapping read pairs that indicate junctions of rearrangements are shown in red. Coverage changes are consistent with 6 fold copy number variation, and coverage depth is variable across the region, consistent with multiple independent breakpoints indicated by the paired end read information.

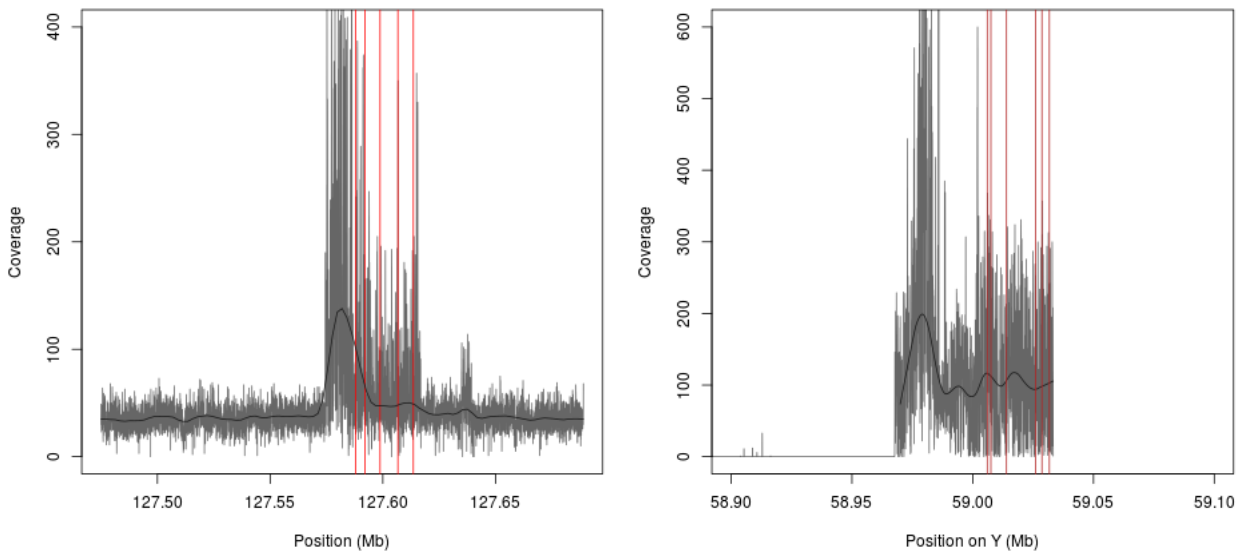

(A) (B)

Figure S5: Genomic coverage with lowess smoothed regression line at the site of a rearrangement (A) at the *Fank1*locus and (B) on the translocated segment of the Y in Denisovan. Locations of abnormally mapping read pairs that indicate junctions of rearrangements are shown in red.

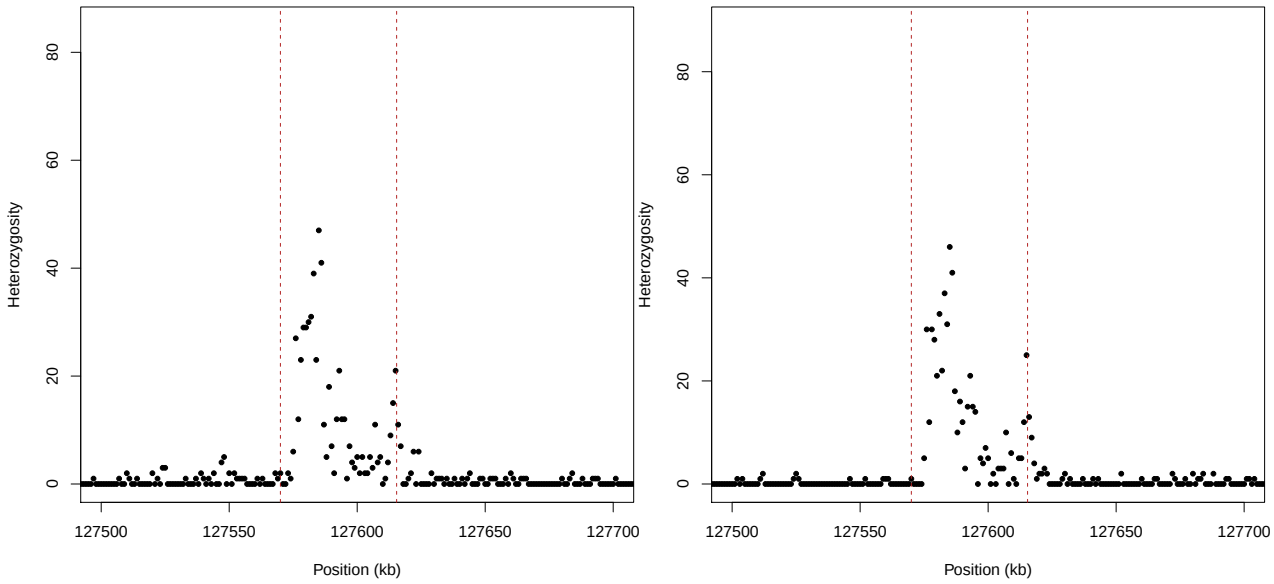

(A) (B)

Figure S6: Heterozygosity for 1 kb windows surrounding the duplicated first exon of *Fank1* in (A) Neanderthal and (B) Denisovan. Boundaries of the duplication inferred from coverage data and abnormally mapping read pairs is shown in red. Heterozygosity for the region is abnormally high, a signature of paralogs accumulating mutations and diverging over time. Heterozygosity is highest in the regions with higher copy number status and return to normal levels outside the duplicated region in *Fank1*.

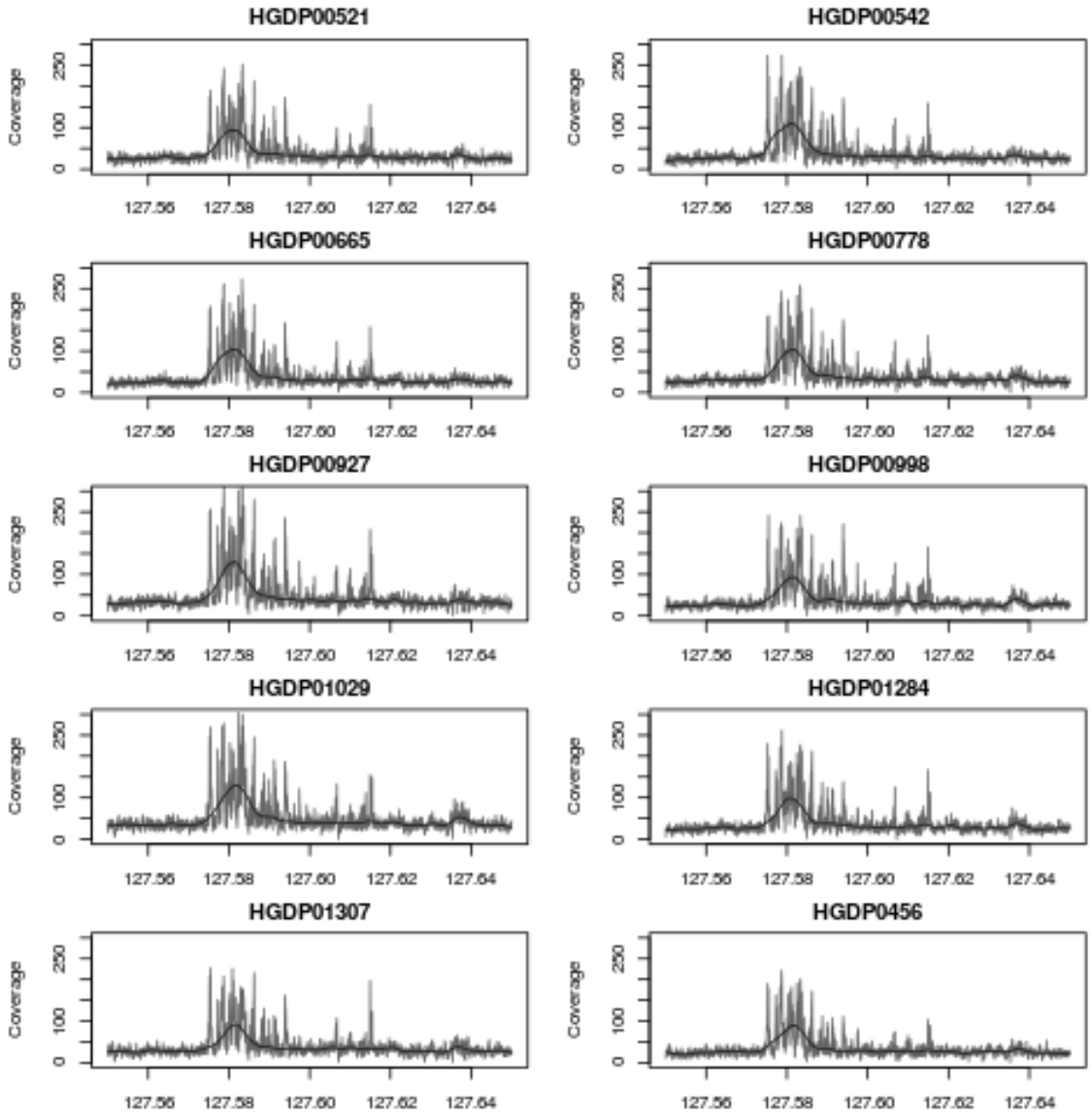

Figure S7: Genomic coverage depth for the translocated segment of the chromosome 10 for 10 modern human genomes. Modern humans show increased coverage consistent with multiple copies for the region.

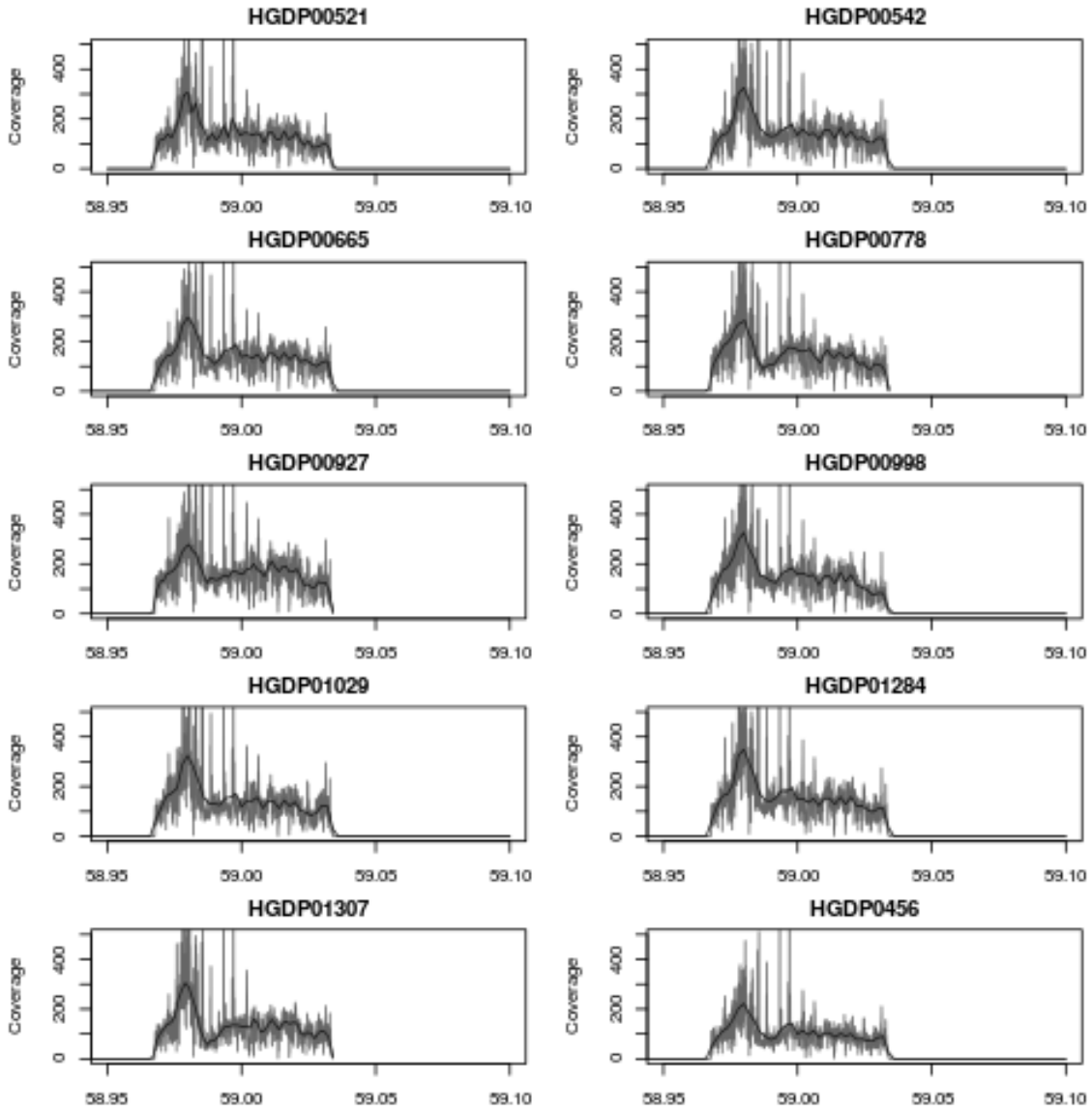

Figure S8: Genomic coverage depth for the translocated segment of the Y in 10 modern human genomes. Modern humans show increased coverage consistent with multiple copies for the region.

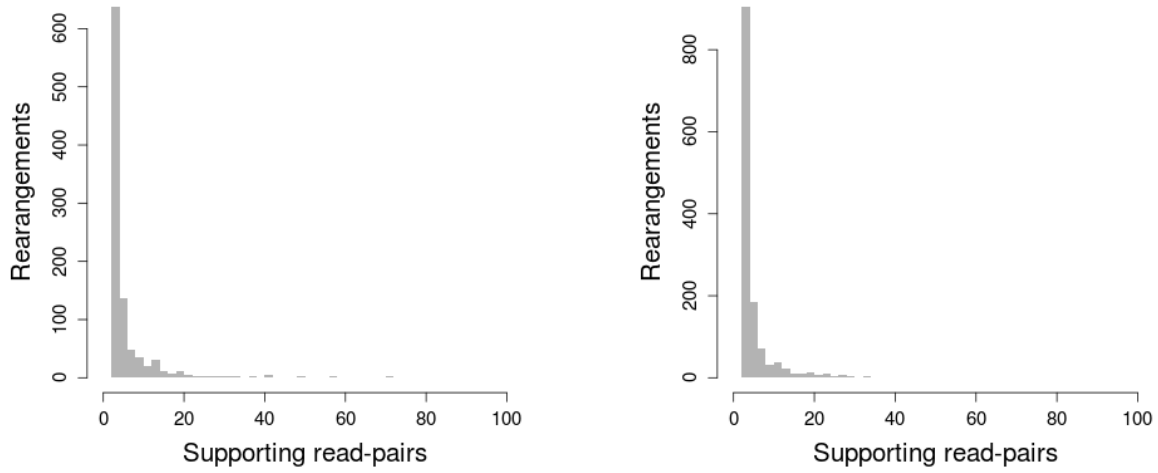

(A) (B)

Figure S9: Read pairs supporting genome structure changes identified in (A) Neanderthal and (B) Denisovan genomes.